Mass Normalized Mode Shapes Using Impact Excitation and Continuous-Scan Laser Doppler Vibrometry

Matthew S. Allen[1] and Michael W. Sracic
Department of Engineering Physics, University of Wisconsin-Madison
535 Engineering Research Building, 1500 Engineering Drive, Madison, WI 53706
[1]Email: msallen@engr.wisc.edu

ABSTRACT:

Conventional scanning laser Doppler vibrometer (LDV) systems cannot be effectively employed with impact excitation because they typically measure a structure's response at only one point at a time. This necessitates exciting the structure at multiple points to create a multi-input-single-output modal test data base, which is not only tedious, but prone to errors due to variations in the impact characteristics from one point to the next. Previous works [1, 2] have demonstrated that an LDV can be used to measure the mode shapes of a structure over a surface by scanning the laser spot continuously as the structure's response decays. The author recently presented a procedure [3] that allows one to post-process continuous-scan LDV (CSLDV) measurements of the free decay of a structure using standard modal parameter identification techniques. Using this approach, one can find the natural frequencies, damping ratios and mode shapes of a structure at hundreds of points simultaneously from a few free responses. The procedure employs a novel resampling approach to transform the continuous-scan measurements into pseudo-frequency response functions, fits a complex mode model, and then accounts for the time delay between samples to obtain the mode shapes. This paper extends the previous work by presenting an algorithm that uses the input force spectrum, measured by an instrumented hammer, to mass normalize the mode shapes obtained using the continuous-scan LDV process. Other issues such as the effect of the scan frequency on the procedure and on speckle noise are also briefly addressed.

1. INTRODUCTION

One significant drawback of conventional scanning laser Doppler vibrometer (LDV) systems is that they only measure the response at one point on a structure at a time. While this limitation is easy to accept for traditional transducers such as accelerometers, which must be bonded to a structure, it seems that there must be a better way to employ an LDV because the laser spot is so easy to reposition. Using the conventional LDV approach, the measurements must be repeated at each point on the structure to obtain the mode shapes of the structure. This point by point approach may be inaccurate if properties of the structure change with time, temperature or other environmental parameters, or if one wishes to use inputs that are difficult to replicate, such as blast or impact loads. Furthermore, it may take quite a long time to acquire measurements at many points on a structure if those points must be acquired one at a time, particularly if the structure has lightly damped, low frequency modes. This may significantly increase the cost of the dynamic test, or one may even be forced on to turn to conventional measurement transducers that are cheaper to use in parallel, even though they are more labor-intensive to set up and may mass load the structure.

In light of these limitations, some researchers have suggested sweeping the laser spot continuously over the structure while measuring its response to try to measure the structure's mode shapes and natural frequencies simultaneously. Sriram *et al.* appear to have been the first to suggest this in the early 1990's [4-6]. Unfortunately, their methods were only marginally successful, and they appear to have abandoned the idea a few years later. More recently, Stanbridge, Martarelli and Ewins began investigating a similar concept, coining the term Continuous-Scan Laser Doppler Vibrometry (CSLDV). They have developed a number of novel methods of extracting one and two-dimensional operating deflection shapes from harmonically excited structures [2, 7-9]. Their methods are elegant, but they require that the structure vibrate at only one frequency, so test times may still be long if one desires to find the structural response at many frequencies, for example if many modes are to be extracted. Their method currently extracts only the operating shape of the structure, so one may encounter difficulty if the structure has modes with close natural frequencies. Perhaps the largest barrier to adopting their methods is that one may simply employ fast sine-fit algorithms, such as Polytec®'s FastScan, when harmonic excitation is used, so it is not clear that CSLDV significantly reduces test times in this scenario [9]. Even if they are not necessarily faster, the CSLDV method does seem to give more accurate mode shapes because it tends to give smooth, continuous mode shapes whereas the mode shapes obtained using the conventional method tend to have glitches at certain points. Vanlanduit *et al.* [10] also presented a CSLDV method that works in conjunction with multi-sine excitation so long as the scan pattern is periodic. Their method repeats the multi-sine input signal an integer number of times, causing the mode shape information to be modulated to

frequencies other than the excitation frequencies. Their approach is quite elegant, but it does require that the laser scan speed, input and response are carefully synchronized, and again the test time may not be much shorter than traditional LDV. All of these approaches require a contacting exciter, such as an electromagnetic shaker, so the structure can be driven harmonically, but that type of exciter may mass-load or otherwise modify the structure, perhaps defeating the purpose of using a non-contact measurement transducer in the first place.

CSLDV can also be applied to identify the modes of a structure from its free or impulsively excited response. This is particularly attractive because hammer tests are so easy to set up, but also because one can identify a number of modes, including mode shapes with high spatial resolution, all from a single free-response. Stanbridge and his associates were the first to apply CSLDV to impact excitation [1, 8, 11], and have revisited the technique recently [12]. They scan the LDV spot sinusoidally while measuring the free-response of the structure. The theory reveals that the spectrum of the CSLDV measurement contains clusters of peaks near each of the natural frequencies of the structure; each mode appears as a collection of pseudo-modes, whose amplitudes can be used to reconstruct a series expansion of the mode shape. Their recent work shows very promising results, especially when the structure of interest is lightly damped and has high natural frequencies. The main disadvantages of their method are:

- The method fails if the structure has low frequency modes, heavily damped modes, or high modal density. In these cases the clusters of peaks describing each mode overlap so one cannot distinguish them.
- The spectrum of the CSLDV signal is complicated, and specialized analysis techniques are required to extract the polynomial representation of the mode shapes from the spectral information.
- Because the mode shapes are represented as polynomial functions, there may be convergence issues or difficulty in dealing with nonstandard geometries.

The impetus for CSLDV is largest for structures with low natural frequencies, because these structures require very long measurement times using traditional scanning LDV, but current CSLDV methods are not easily applied to these structures because of the requirement that the scan frequency be low relative to the modal separation. The importance of the second bullet must also not be overlooked. For example, Figures 3 and 4 show the spectra of one of the CSLDV measurements obtained in this work. Dozens of peaks appear in the spectra, some of which are physical and others that are due to measurement noise. Processing a measurement such as this would be difficult without specialized mathematical software, and even visual troubleshooting requires considerable effort and expertise. (One could, in principle, apply standard modal parameter identification routines to the CSLDV response and extract the multitude of pseudo-modes in the response, but this would entail using high order matrix polynomials [13], which are computationally expensive and introduce numerical ill-conditioning.)

The method employed here overcomes many of these limitations, greatly expanding the range of systems to which CSLDV can be applied. This method also allows one to use standard modal analysis procedures to extract the modal parameters from the data, to detect modes with close natural frequencies, and to visually interrogate the data. There are also some advantages with regards to laser speckle noise; this method collects all of the speckle noise to a single frequency line in the response. The proposed approach is also easily expanded to multi-input-multi-output (MIMO) data sets. Once the LDV is set up, one can simply strike the structure at a number of different locations, record the response with the CSLDV, and process the measurements as if they were traditional MIMO measurements.

This method was first presented by the authors in [3], but it is based on algorithms developed for rotating systems that were presented some time earlier [14-16]. The basic idea is to resample the measurements synchronous with the scan frequency, creating a response in which the laser spot is at one of a finite number of points on the structure at each time instant. The samples corresponding to each point can then be collected and processed as if all points had been measured simultaneously, using standard, state-space MIMO modal identification techniques. A post-processing step accounts for the phase delay between each measurement point. The resulting mode shapes capture the motion of the structure at hundreds of points along the scan path, so the density of the information obtained is hundreds of times higher than would be obtained by conventional LDV in the same amount of time, and is limited only by the noise in the signal and the sample rate of the LDV. The shapes are also more consistent than would be obtained with conventional impact excitation and LDV, because they are obtained from one free response whereas the conventional approach requires repeatedly exciting the structure, and the input force tends to vary significantly from one scan point to the next because the angle of the hammer blows and the point at which the hammer strikes are difficult to control [12].

This work presents an algorithm by which one can mass-normalize the mode shapes obtained by CSLDV. The scale factors derived using the proposed method agree well with those predicted analytically for a free-free beam, especially considering the inherent uncertainty in the impact excitation. This work also explores the effect of the scan frequency on the data reduction process and the quality of the measurements and demonstrates the proposed method on a structure that has

relatively high frequency modes compared to the scan frequencies that the LDV is capable of. Good results are obtained even in this extreme case.

The following section reviews the theory presented in [3] and presents the proposed mode vector scaling routine. Section 3 applies these methods to a free-free beam in a laboratory setup, followed by conclusions in Section 4.

2. THEORY

The method used in this work to find the mode shapes and natural frequencies from CSLDV measurements was originally developed by Allen and Ginsberg [14] to identify parametric models of linear time-periodic systems such as cracked shafts, rotating tires and other anisotropic rotating systems. It was later extended by Allen in [15, 16]. Allen and Sracic [3] recently applied the methods to identify the mode shapes and natural frequencies of a structure from CSLDV measurements. Some of the theory presented in [3] will be highlighted in Section 2.1, following which the mode shape scaling method will be presented in Section 2.2.

2.1 Modal Analysis of CSLDV Measurements Using the Multiple Discrete Time Systems Method

The signal $y(t)$ measured by a scanning LDV on a freely vibrating, linear, time-invariant structure, can be expressed as a sum of decaying exponentials in terms of the state space modal parameters of the structure as follows

$$y(t) = \sum_{r=1}^{2N} \phi(x,y,z)_r \, D_r e^{\lambda_r t}$$
$$\lambda_r = -\zeta_r \omega_r + i\omega_r \sqrt{1-\zeta_r^2} \;\; , \;\; \lambda_{r+N} = -\zeta_r \omega_r - i\omega_r \sqrt{1-\zeta_r^2} \tag{1}$$

where λ_r is the rth complex eigenvalue, which is expressed in terms of the rth natural frequency ω_r and damping ratio ζ_r. The corresponding mode vector $\phi(x,y,z)_r$ depends on the position of the laser beam along its path, which could involve motion in three dimensions in general, although typical single-point LDVs measure only the portion of the structure's velocity that is parallel to the laser beam, so a two-dimensional path is more likely to be employed. D_r is the complex amplitude of mode r, which depends upon the structure's initial conditions, which in turn depend on the impulse used to excite the structure.

The laser is assumed to traverse a known, periodic path of period T_A, such that $x(t) = x(t+T_A)$, $y(t) = y(t+T_A)$, and $z(t) = z(t+T_A)$. The scan frequency is $\omega_A = 2\pi/T_A$. Because x, y and z are all periodic with the same period, the mode shape modulating the exponential is also periodic, so

$$y(t) = \sum_{r=1}^{2N} \phi(t)_r \, D_r e^{\lambda_r t}$$
$$\phi(t)_r = \phi(t+T_A)_r \tag{2}$$

One can eliminate the time dependence of the mode shapes in eq. (2) by sampling an integer number of times per scan period T_A. (In practice this can be achieved by resampling the CSLDV signal synchronous with the scan frequency.) The number of samples per period is denoted N_o because the resulting time signal contains the response at N_o discrete points, so that integer is also the number of output measurement locations. The sample increment is $\Delta t = T_A / N_o$. Current LDV systems are capable of sampling at rates of up to a few MHz, thousands of times faster than realistic scan rates $1/T_A$, so N_o can be quite large. The CSLDV signal is then separated into N_o different sampled responses as follows.

$$\begin{aligned}
y_0 &= [y(0), y(T_A), y(2T_A), \cdots] \\
y_1 &= [y(\Delta t), y(\Delta t + T_A), y(\Delta t + 2T_A), \cdots] \\
y_2 &= [y(2\Delta t), y(2\Delta t + T_A), y2(\Delta t + 2T_A), \cdots] \\
&\cdots \\
y_{N_o-1} &= [y((N_o-1)\Delta t), y((N_o-1)\Delta t + T_A), y((N_o-1)\Delta t + 2T_A), \cdots]
\end{aligned} \tag{3}$$

Because the scan frequency is synchronous with the sample frequency, each of these responses corresponds to a particular point along the scan path. This is the essence of the Multiple Discrete Time Systems (MDTS) method [16]. The time dependence of the mode shape in eq. (2) has been eliminated, so each of these responses is identical to the free response that one would measure at each position if the laser spot were held stationary at that location. These responses can be transferred to the frequency domain using the Discrete Fourier Transform (DFT or FFT), resulting in a set of pseudo-Frequency

Response Functions (FRFs). The term pseudo is used because the residues in eq. (2) (and in its Fourier transform) differ from the residues of a true FRF by a scale factor. In other respects these pseudo-FRFs can be treated as traditional FRFs. A collection of these responses for various initial times spanning $(0,T_A]$ share the same eigenvalues, differing only in their modal amplitudes, so they can be processed using a global parameter identification routine to find the system's eigenvalues and mode shapes (up to a scale factor D_r). The resulting mode shapes encompass all of the points that the laser has swept during the time response. One can also incorporate additional measurements to minimize errors and address close natural frequencies, analogous to what is done for linear time invariant systems. For example, input at a different point would likely change the proportionate contribution of the modes and hence their constants D_r, so the set of responses due to different inputs can be treated as an additional column of the pseudo-FRF matrix and processed appropriately to identify modes with close natural frequencies [17-19].

One will notice that the responses in eq. (3) are not sampled at the same time instants, so one must account for the time delay between each spatial sample to obtain accurate mode shapes, as discussed in the appendix of [14] and in [15].

It is important to recognize that the MDTS procedure has the effect of aliasing any natural frequencies above $\omega_{max} = \omega_A/2$. Modes with natural frequencies higher than ω_{max} appear at lower frequencies in the MDTS responses. Ideally, one would scan the laser spot over the structure of interest quickly such that ω_{max} is greater than the highest frequency of interest. Current galvo-mirror systems are capable of scanning at rates of 500 Hz or more, so this may often be possible. If the scan frequency is lower than the highest natural frequency of the structure, the natural frequencies identified while processing the MDTS responses will be aliased. In that case, the true natural frequencies can be obtained by performing a point measurement (or a small number of point measurements) to supplement the CSLDV measurements. The authors have also found that one can usually determine the true natural frequencies from the aliased ones using a simple, automated algorithm that adds various integer multiples of ω_{max} to the identified eigenvalues and searches for that which gives in the greatest modal phase co-linearity when post processing the mode shapes to account for the phase delay between measurement points ([14, 15]). For lightly damped structures such as the beam used in the following section, this has proven to be a very robust way of determining the true (unaliased) natural frequencies.

2.2 Mode Shape Scaling Theory

The residue matrices obtained using the MDTS procedure are proportional to the mode shapes, but the scale factor D_r is not known. This section shows how one can mass normalize the mode shapes if the impulse exciting the structure has been measured, for example, if an instrumented hammer was used to excite the structure. The standard procedure when employing hammer excitation is to trigger based on the hammer signal and record the response of the system from just before the start of the excitation until the excitation decays. The hammer signal is short, so the structure responds freely for most of the time window. The procedure described in the previous subsection is applied to the free response of the structure, which is found by deleting that portion of the response that occurs before the force has ceased. Because the hammer signal has been recorded, one is free to restore the forced portion of the response and use the measured force to scale the mode vectors. To do so, consider the familiar frequency domain input-output, transfer function relationship of a linear time invariant system between all outputs Y and a single input U:

$$\underset{N_o\times 1}{\{Y(\omega)\}} = \underset{N_o\times 1}{\{H(\omega)\}}U(\omega) \tag{4}$$

If the structure is lightly damped or proportionally damped, then its mode vectors are well approximated as real and the frequency response function takes the following form

$$\{H(\omega)\} = \sum_r^N \frac{\{\phi_r\}\phi_{r,dp}}{\omega_r^2 - \omega^2 - 2i\omega\zeta_r\omega_r} \tag{5}$$

where $\{\phi_r\}$ is the rth mass normalized mode vector at N_o output points, $\phi_{r,dp}$ is the mode shape at the drive point, and N is the number of modes needed to represent the response in the frequency band of interest.

All of the parameters in eq. (5) can be found using the method in the previous section except for the scale factor between the experimentally identified mode shapes and the mass normalized mode shapes that appear in eq. (5). The factor of proportionality for the rth mode is denoted C_r so that

$$\{\phi\}_r = C_r\{\phi_{r,ex}\}, \tag{6}$$

where $\{\phi_{r,ex}\}$ denotes the rth unscaled mode shape found experimentally by CSLDV and $\{\phi_r\}$ is the corresponding mass normalized mode shape. The mode shapes found from the free responses are also proportional to the mass normalized shapes, but with a constant of proportionality D_r, which depends on the initial conditions. The constant is used here will be related to the force which occurred at an earlier time and caused the initial conditions upon which D_r depended.

Turning our attention to the drive point residue, recall that the mode shapes are defined on output points that are not explicitly chosen, but are a result of the scan pattern chosen ($x(t)$, $y(t)$, $z(t)$) and the sample rate of the LDV. One can find the drive point mode shape in $\{\phi_{r,ex}\}$ so as long as the drive point location was traversed in scan and its (x, y, z) location is known. One can then find the output point that most closely corresponds to that location and use its value for the drive point mode shape. A more robust approach involves fitting a low-order polynomial to the mode shape near the drive point and using the polynomial to extract the drive point mode shape. In this study, a line was fit to a few mode shape coefficients near the drive point to determine the drive point mode shape. Substituting eqs. (6) and (7) into (5) one obtains

$$\{Y(\omega)\} = \sum_r^N \frac{C_r^{\,2}\{\phi_{r,ex}\}\phi_{r,ex,dp}U(\omega)}{\omega_r^2 - \omega^2 - 2i\omega\zeta_r\omega_r} \tag{7}$$

The only unknowns in the equation above are the squared scale factors C_r^2, which appear linearly. The input and output are known at many frequencies, so a linear least squares problem can be formulated to find the unknown scale factors. However, the output is only measured at each output point once per scan cycle, so the equation above must be modified slightly to account for this. Taking the inverse Fourier transform of both sides of the equation, and then recognizing that the CSLDV signal at time $t_k = k\Delta t$ depends on the mode shape a the kth measurement point $\left(\phi_{r,ex}\right)_k$, one obtains the following.

$$\begin{aligned} y_{CSLDV}(t_k) &= \sum_r^N C_r^2 \left(\phi_{r,ex}\right)_k q_r(t_k) \\ q_r &= \phi_{r/dp,ex}\, IDFT\left(\frac{U(\omega)}{\omega_r^2 - \omega^2 - 2i\omega\zeta_r\omega_r}\right) \end{aligned} \tag{8}$$

The response of the rth modal coordinate to the input at the kth time instant is denoted $q_r(t_k)$, and is found by dividing the input spectrum by the familiar denominator, which is constructed from the identified modal natural frequency and damping ratio, and then performing an inverse Discrete Fourier Transform (such as MATLAB's '*ifft'* function).

The signals on both sides of this equation can be separated into N_o separate responses, corresponding to each output location, as was done in eq. (3), resulting in N_o CSLDV responses $y_{CSLDV,p}$ for $p = 1 \ldots N_o$. One also obtains N_o modal responses $q_{r,p}$, for each mode r and each output point p. The pth response is given below in matrix form where N_c denodes the number of time samples per output point.

$$\begin{aligned} \{y_{CSLDV,p}\} &= \begin{bmatrix} \phi_1(t_p)\{q_{1,p}\} & \cdots & \phi_N(t_p)\{q_{N,p}\} \end{bmatrix} \begin{bmatrix} C_1^2 \\ \vdots \\ C_N^2 \end{bmatrix} \\ \{y_{CSLDV,p}\} &= \begin{bmatrix} y_{CSLDV}(t_p) & y_{CSLDV}(t_p + T_A) & \cdots & y_{CSLDV}(t_p + N_c T_A) \end{bmatrix}^T \\ \{q_{r,p}\} &= \begin{bmatrix} q_r(t_p) & q_r(t_p + T_A) & \cdots & q_r(t_p + N_c T_A) \end{bmatrix}^T \end{aligned} \tag{9}$$

The modal scale factors are the same for all output points, so these equations can be stacked resulting in a linear least squares problem for the unknown C_r^2 values. It is more convenient to solve this least squares problem in the frequency domain so one has the option of excluding any frequency bands that are dominated by narrow-band noise (e.g. speckle noise [20-22]). Denoting the FFT of each signal with a capital letter, the complete frequency-domain least squares problem is then

$$\begin{bmatrix} \{Y_{CSLDV,1}\} \\ \vdots \\ \{Y_{CSLDV,N_o}\} \end{bmatrix} = \begin{bmatrix} \phi_1(t_1)\{Q_{1,1}\} & \cdots & \phi_N(t_1)\{Q_{N,1}\} \\ \vdots & \vdots & \vdots \\ \phi_1(t_{N_o})\{Q_{1,N_o}\} & \cdots & \phi_N(t_{N_o})\{Q_{N,N_o}\} \end{bmatrix} \begin{bmatrix} C_1^2 \\ \vdots \\ C_N^2 \end{bmatrix}. \tag{10}$$

The size of the first matrix in the right hand side of the least squares problem is (N_o*N_f) by N where N_f specifies the number of frequency lines used per output location. Computation time can be substantially reduced by using only the frequency data near the peak of each mode, for example in the modal half power bandwidth, as described in [23]. This also reduces the sensitivity of the least squares problem to narrow-band noise, as Ginsberg *et al.* showed in [24].

3. EXPERIMENTAL RESULTS

The CSLDV method was applied experimentally to the same free-free aluminum beam discussed in [3]. Figures 1 and 2 below describe the experimental setup. The beam was suspended in a frame and secured by soft bungee cables to limit rigid body motion. The natural frequencies of the two most important rigid body modes were below 3Hz, while the first bending mode occurs at 17 Hz.

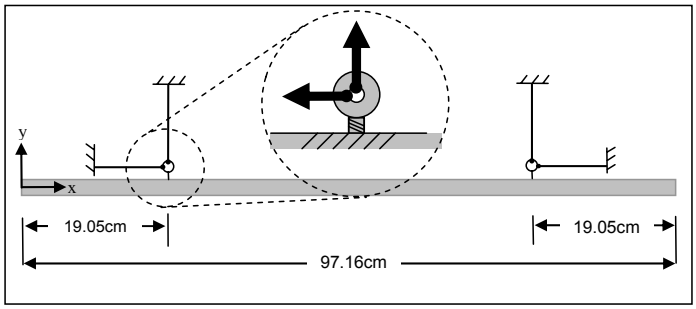

Figure 1: Schematic and dimensions of test setup

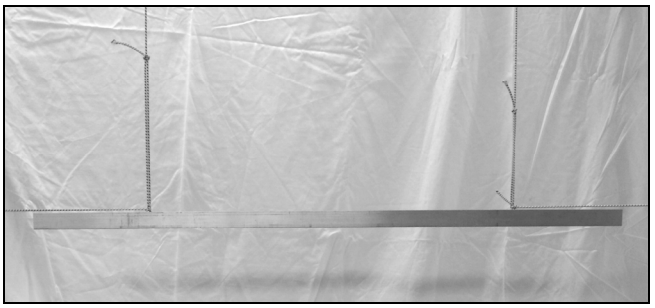
Figure 2: Aluminum beam and support system

The beam was excited using an impulse hammer (PCB Piezotronics modally tuned ICP impact hammer 086C01) at five inputs located at x-positions equal to 55.9 cm, 62.9 cm, 70.5 cm, 78.1 cm, and 85.73 cm with respect to the datum shown in Figure 1. The CSLDV method was employed to measure the beam's transient response for each input by driving the mirrors in a Polytec® PSV-400 scanning laser vibrometer at sinusoidal scan frequencies of 21 Hz, 51 Hz, and 100 Hz in the x-direction. The mirrors were controlled by supplying a sinusoidal signal to the mirrors using a custom cable between the LDV head and the data acquisition computer. The vibrometer's data acquisition system was utilized to record the force signals and the driving voltage signal. The drive signal was generated using a Tektronix AFG 3022 dual channel arbitrary/function generator.

The Polytec software does not allow one to calibrate the position of the laser spot to the video image when the custom driving voltage is present, so a different approach was employed. If one assumes that the driving voltage and laser position are related by a linear dynamic system, then the following relationship must hold for a sinusoidal scan speed of $f_{scan} = 2\pi\omega_A$

$$X(f_{scan}) = G(f_{scan})V(f_{scan}). \tag{11}$$

The driving voltage magnitude was manually adjusted until the laser traversed all but a few millimeters of the ends of beam. The laser's position on the beam as a function of time was determined by recording the driving voltage of the *x*-mirror and the distance from the end of the scan pattern to the end of the beam. A significant delay was discovered between the function generator's input signal and the mirror's response. This was corrected manually by searching for the phase lag for which the same mode shape was measured on the forward and backward sweeps of the beam [3]. Ideally, these operations would be avoided in the future by simply taping the position signals for the mirrors, which are available in the LDV head although difficult to access.

For each input, 25 seconds of response data was recorded at 20 kHz. The sample rate appeared to be more than sufficient to capture all of the frequency content that stood out above the noise floor. An exponential window with a decay constant of $0.20s^{-1}$ was then applied to the vibrometer signal to reduce the effects of leakage and noise. This was approximately equal to the minimum decay constant of any of the elastic modes, which was shown to be optimum in [19] when an impulse response is contaminated with Gaussian noise.

3.1 Experimental CSLDV Results Using MDTS Method

Figures 3 and 4 show the frequency domain spectrum of a CSLDV measurement before processing by the MDTS method. The scan frequency was 51 Hz. The complexity of the full CSLDV signal is immediately apparent from the multitude of peaks. Peaks are present near each of the modal frequencies, and at integer multiples of the scan frequency and the modal frequencies, as discussed in [3]. This is easiest to see in Figure 4, which shows an expanded view of only part of the spectrum. Laser speckle noise also appears at some harmonics of the scan frequency, most noticeably at 51 and 102 Hz in Figure 4.

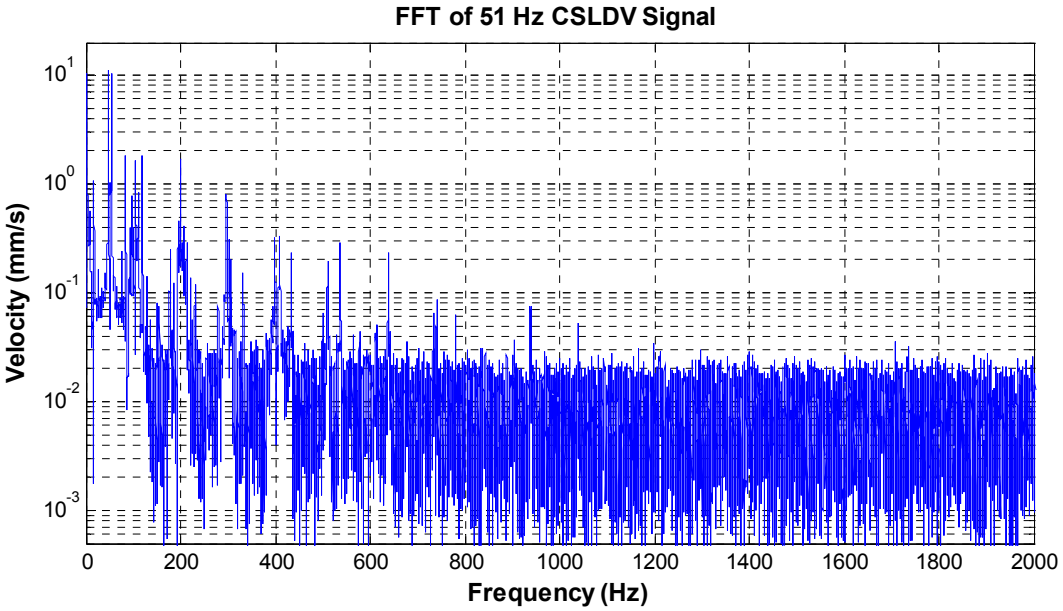

Figure 3: FFT of CSLDV signal for input DP-5 at x = 78.1 cm

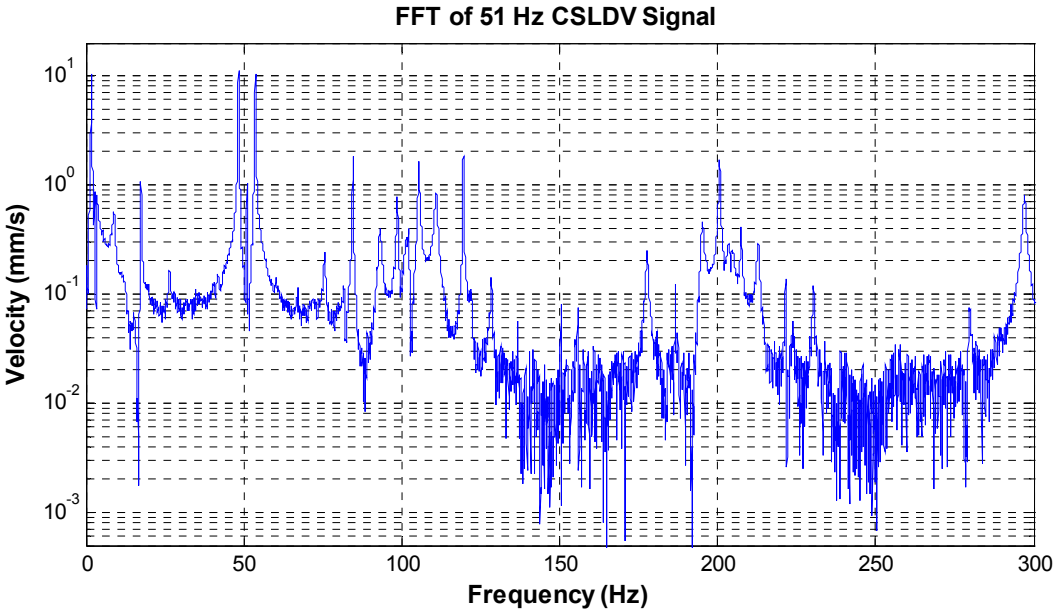

Figure 4: Expanded view of CSLDV signal in Figure 3

In order to utilize the MDTS method, the portions of the measured signals before and during the force pulse were deleted leaving only the free-response of the beam. Because the clocks between the function generator and the data acquisition system were not precisely synchronized, the measured signals were resampled using a simple algorithm, as discussed in [3]. The frequency of the mirror drive signal, as recorded by the data acquisition system, was found to be 51.0004 Hz, and this

more precise value was used to resample the force, response and mirror drive signals. Following resampling, the full response signals were decomposed into spatial outputs as explained by eq. (3), and transformed into the frequency domain using an FFT to give a 5 input and 402 response point, 644 frequency line pseudo-FRF matrix. The laser sweeps a forward path and then returns along the same trajectory for the line scan employed here, so some of the 402 measured response points may be replicates. The complex mode indicator function (CMIF), shown in Figure 5, was formed for the 5-input set of MDTS responses, to see whether any repeated natural frequencies exist.

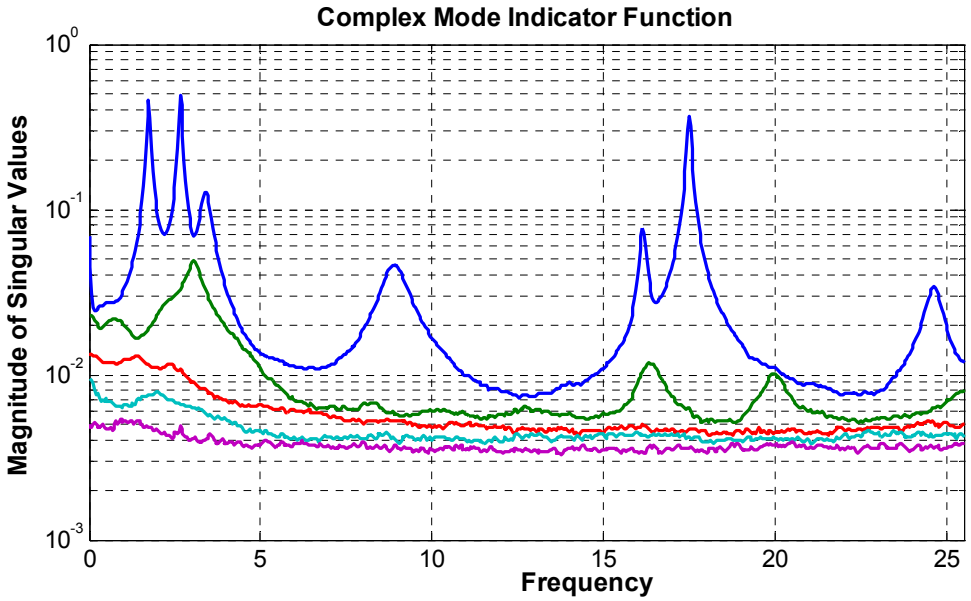

Figure 5: Complex Mode Indicator Function (CMIF) of CSLDV data after processing by MDTS method

The CMIF shows that the MDTS procedure has resulted in a much simpler spectrum than the original CSLDV spectrum in Figures 3 and 4. The reason for this is that all of the harmonics corresponding to each mode, which cluttered the full spectrum CSLDV signal, have been folded onto one peak in the MDTS responses. The CMIF essentially averages over all pseudo-points, so the result is a clean spectrum showing one peak per mode of the beam.

A CMIF is not really needed for a simple system like a free-free beam, whose modes all have distinct natural frequencies, but in this case it is somewhat useful because of aliasing. The hammer excites modes well beyond f_{max} (25.5 Hz in in this case), so most of the bending modes are aliased to lower frequencies. The CMIF reveals nine peaks residing below 25.5 Hz but only three of these peaks correspond to frequencies with values that are truly less than 25.5 Hz. Aliasing is best visualized as folding of the modal peaks about f_{max} and 0. For example, the beam's second bending mode at about 48 Hz folds back across f_{max} and appears to reside at 25.5 - (48 - 25.5) = 3.0 Hz. Frequency content at 60 Hz would fold twice and appear at 0 + (60 - 2*25.5) = 9 Hz. The second singular value trace in the CMIF (green) always has a considerably lower magnitude than the first, suggesting that none of the (aliased) frequencies in the pseudo-FRFs are repeated. If this were not the case, the measurement could be repeated with a different scan frequency until all of the frequencies were reasonably distinct.

As discussed previously, it would be ideal to scan the mirrors at a much higher frequency than the maximum frequency of interest. However, the scanning mirrors on the PSV-400 are internal to the head and would be expensive to repair, so high frequencies were avoided because the maximum safe operating frequency of the head was not known. Furthermore, the mirrors seem to respond nonlinearly to the drive voltage at higher scan frequencies so eq. (11) could no longer be applied to estimate the mirror angle. Some of these issues could have been addressed fairly easily, but for the present work we limited ourselves to scan frequencies below 100 Hz. An additional motivation of using such a low scan frequency was to demonstrate the surprisingly benign effect that severe aliasing had on the experimental results for this system. On the other hand, higher scan frequencies would be necessary for systems that have higher modal density than this simple beam.

Figure 6 shows the mode shapes obtained by AMI from the CSLDV data for a 51 Hz scanning frequency. The response was sampled at 20,480 Hz, and resampled at 20,502 Hz so the shapes were actually estimated at 402 pseudo-measurement points. As Stanbridge *et al.* [12] have pointed out, the actual resolution of the data is determined by the number of Fourier coefficients that are significant in the response, so not all of the points are significant. On the other hand, including a surplus of measurement points allows one to average out experimental scatter to some extent. The experimental shapes agree very well with the analytical shapes, except perhaps for the seventh bending mode (428 Hz). The seventh bending mode, appearing as mode 9 in Figure 6, has especially large errors near the right end of the beam.

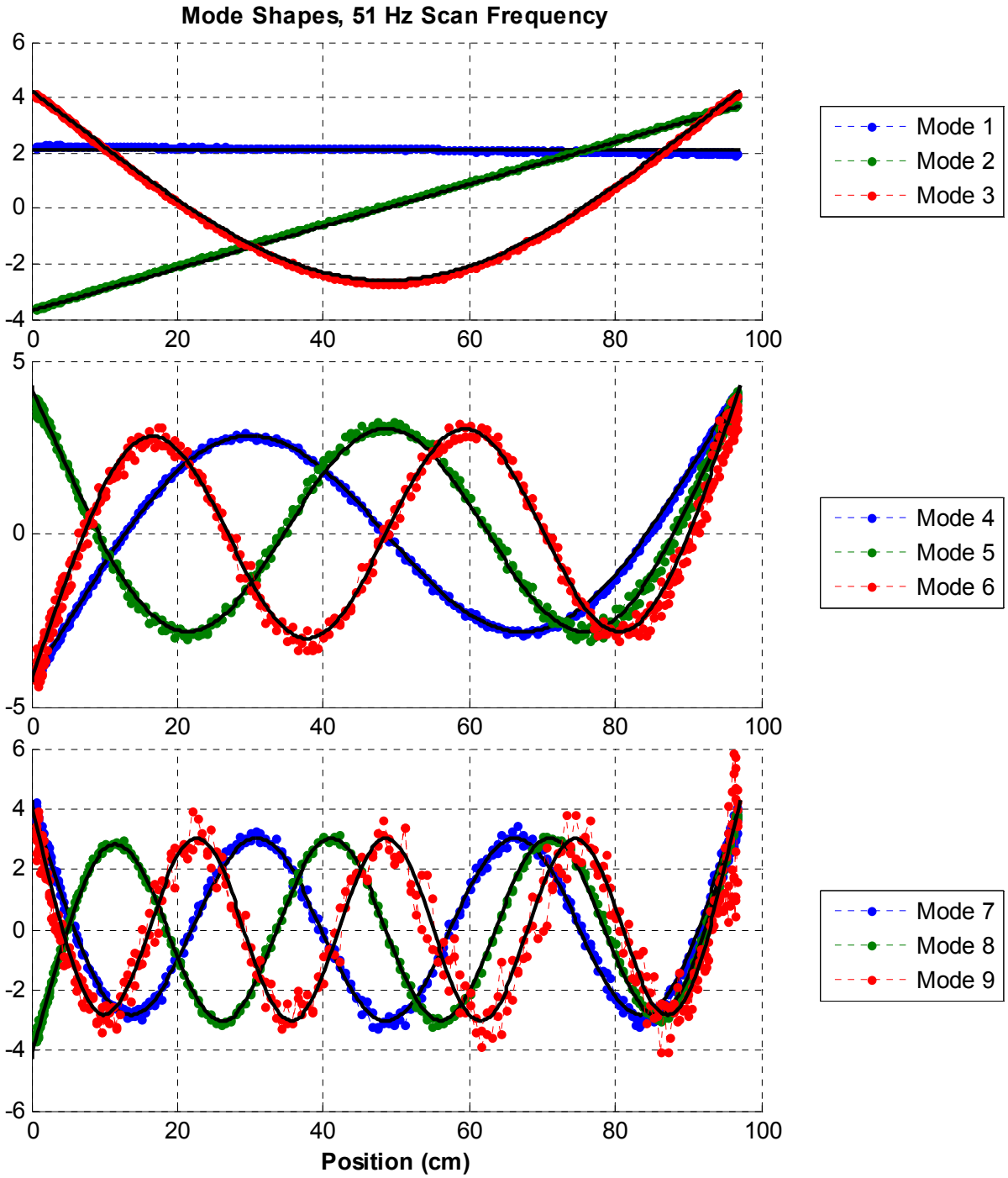

Figure 6: Mode shapes for free-free beam obtained experimentally using CSLDV with 51Hz scanning frequency, compared to analytical shapes. Solid black lines denote the analytical Euler-Bernoulli shape; dots show the experimentally obtained shapes at each pseudo-measurement point. The experimental mode vectors shown here were scaled to have the same norm as the analytical ones, so only the shapes of the vectors is of interest in this plot.

3.2 Experimental Mass Normalization

The procedure described in Section 2.2 was applied to find the unknown scale factors C_r relating the identified mode shapes to the mass-normalized mode vectors. The unscaled shapes, shown in Figure 6, were used in the procedure along with the unaliased natural frequencies and damping ratios shown in Table 2. Recall that these mode shapes were obtained by applying MIMO system identification to the 5-input response set. The AMI algorithm that was used in this process considers all of the inputs simultaneously and identifies a rank-one residue matrix for each mode. Each column of that residue matrix is

proportional to the same mode shape, so that shape, whose scale factor was arbitrary, was used in the normalization procedure.

The data used in the normalization procedure was exactly the same as that used by AMI in the modal identification procedure, except that the responses used by AMI omitted the portion that occurred before and during the input. We return to the full measured time histories, which include the force pulse, to perform the scaling.

Two different approaches were used to scale the mode shapes. First, each measured hammer force and corresponding multi-output CSLDV response was treated separately. Each pair of input-output data was used to solve the least squares problem in eq. (10), and the scale factors were stored. The second approach stacked the least squares problems for all five input points, resulting in a large overdetermined system of linear equations, which were solved to find the scale factors that best satisfied the entire data set. While this least squares problem was large (the matrix on the right in eq. (10) had 265,320 rows and 9 columns) the computation required less than a second in Matlab so the operation was not particularly expensive.

The scale factors C_r were used in eq. (6) to find the experimentally estimated, mass-normalized mode vectors $\{\phi\}_r$. The Modal Scale Factor (MSF) was then computed between these vectors and the analytical mass normalized mode vectors, obtained using Euler-Bernoulli beam theory. The analytical mode vectors were denoted $\{\phi\}_{r,an}$. The definition for the MSF follows, based on [25].

$$MSF_r = \left| \frac{\{\phi\}_r^T \{\phi\}_{r,an}}{\{\phi\}_{r,an}^T \{\phi\}_{r,an}} \right| \tag{12}$$

The modal scale factors for each drive point, and those obtained by the MIMO procedure are shown in Table 1. The five drive points are denoted DP-1 … DP-5, and the x-coordinate of each drive point is also given. The natural frequencies are also listed for convenience. Most of the MSFs for each of the five drive points are near one, indicating good agreement between the scale of the experimental and analytical mode shapes. The variation in the MSFs is usually less than 20%, although some of the MSFs differ by 300% or more at certain drive points. In an effort to explain this discrepancy, the amplitude of the drive point mode shape was found to see whether these poor MSFs might come about due to weak excitation of that mode in that particular drive point. For convenience, the drive point amplitude was normalized by the maximum absolute value of the mode shape, resulting in the normalized drive point amplitude L_r.

$$L_r = \frac{\left|\phi_{r,dp}\right|}{\max\left(\left|\{\phi_r\}\right|\right)} \tag{13}$$

The normalized drive point amplitude L_r is near one if the drive point excites the rth mode as much as possible and near zero if the excitation is at a node. The L_r values are also shown in Table 1 for each mode at each drive point. All of the MSFs that are greater than 1.5 correspond to drive point amplitudes close to zero. If all of the MSFs corresponding to L_r less than 0.3 are excluded, the scatter in the remaining MSFs is less than 30% for all of the modes. The MSFs obtained using MIMO scaling procedure are also shown in the rightmost column of Table 1. They are all within 10% of the average of the MSFs that have considerable drive point amplitude.

One should note that although an MSF value of one indicates perfect scale agreement between the analytical model and the experiment, the analytical model is only an approximation to the real system, subject to the limitations of Euler-Bernoulli beam theory. The scale of the analytical mode vectors also depends on the density of the beam, which is not precisely known; nominal values were used for the analytical beam's modulus and density. Furthermore, there is potentially a good deal of uncertainty associated with the direction and location of the hammer blows, which may contribute to the variation in the MSFs. Uncertainty in the damping ratio of the each mode may also contribute to the variability.

Freq. (Hz)	DP-1, 55.9 cm		DP-2, 85.7 cm		DP-3, 62.9 cm		DP-4, 70.5 cm		DP-5, 78.1 cm		MIMO
	MSF	*Lr*	MSF	*Lr*	MSF	*Lr*	MSF	*Lr*	MSF	*Lr*	MSF
1.7	1.16	0.9	1.17	0.9	1.11	0.9	1.22	0.9	1.14	0.9	**1.16**
2.7	1.09	0.2	1.18	0.8	0.95	0.3	1.25	0.5	1.15	0.6	**1.16**
17.5	1.10	0.9	1.12	0.5	1.12	0.7	1.01	0.3	1.28	0.1	**1.11**
47.6	0.88	0.4	1.12	0.1	0.92	0.6	1.01	0.7	0.95	0.4	**0.94**
93.1	0.91	0.5	0.88	0.3	3.62	0.0	0.96	0.7	0.88	0.9	**0.91**
153.7	0.87	0.6	0.83	0.5	0.88	0.7	3.14	0.0	0.93	0.6	**0.89**
230.4	1.13	0.3	0.84	0.8	0.72	0.6	0.80	0.5	0.94	0.4	**0.81**
322.1	1.00	0.8	1.01	0.8	1.77	0.1	1.04	0.8	0.54	0.1	**1.03**
428.1	0.42	0.1	0.65	0.7	0.62	0.7	0.77	0.2	0.57	0.3	**0.62**

Table 1: Modal Scale Factors between experimentally scaled mode shapes and analytical for 5 drive points, each taken individually and for the MIMO procedure. 51 Hz CSLDV scan frequency.

3.3 Effect of Scan Frequency

A number of scan frequencies were explored to assess the effect that the scan frequency had on the results. Figure 7 shows the average of the magnitude of the pseudo-FRFs obtained using three different scan frequencies. For example, the 51 Hz data resulted in 402 pseudo-FRFs at each of five drive points, so the average was performed over 2010 pseudo-FRFs. A 20kHz sample rate was used for all of the data sets, so the 100 Hz and 21 Hz data sets had 205 and 976 pseudo-points respectively after resampling. AMI was applied to each of the MIMO data sets, the modes of the beam were identified, and their mode shapes, damping ratios and unaliased natural frequencies were estimated. The marker near each peak in Figure 7 gives the unaliased natural frequency of the mode that was identified at that peak, illustrating the effect that the scan-frequency has on aliasing the natural frequencies. As the scan frequency decreases, the unaliased bandwidth decreases while the number of modes present in the response remains the same, so the modal density seems to increase. Also, it was shown in [3] that aliasing reduces the imaginary part of each modes complex eigenvalue, not its real part, so the damping ratio of each mode appears to increase as the scan frequency decreases. This can make the high frequency modes more difficult to detect. This is exacerbated by the fact that the force spectrum falls off quickly; the Power Spectral Density of the input at 500 Hz (not shown) is less than a hundredth of that at 20 Hz. As a result, the seventh bending mode, at 428 Hz, is the highest mode that is significantly excited.

We emphasize again that in the ideal scenario, the scan frequency would be more than twice the maximum frequency of interest. A scan frequency of at 51 Hz, whose Nyquist rate is 25.5 Hz, is nearly 20 times too small than what would be required to avoid aliasing the 428 Hz mode. At even lower scan speeds the methods of Stanbridge *et al.* [12] might be preferred. To illustrate the difference between these methods, consider the following. The lowest bending mode of this system occurs at 17 Hz, if one must capture 20 harmonics to describe that mode's shape, and assuming that 10 fall on either side of the peak, a scan frequency of 1.7 Hz or less must be used to employ their methods. On the other hand, such a low scan frequency might not even traverse the length of the beam before some of the high frequency modes had vanished, so multiple tests would probably be required at various scan frequencies to identify the first seven elastic modes using their techniques.

Table 2 compares the natural frequencies of the modes identified from the MIMO data at each of the scan frequencies. Both the estimates of the true frequencies (unaliased) and the frequencies at which those are aliased are shown. The estimated true frequencies all agree quite closely. The frequencies of the rigid body modes varied somewhat, as shown in Figure 7, but this was due to variation in the tension of the bungee cords used to suspend the beam. This may also account for some of the differences between the identified frequencies, but the differences are very small.

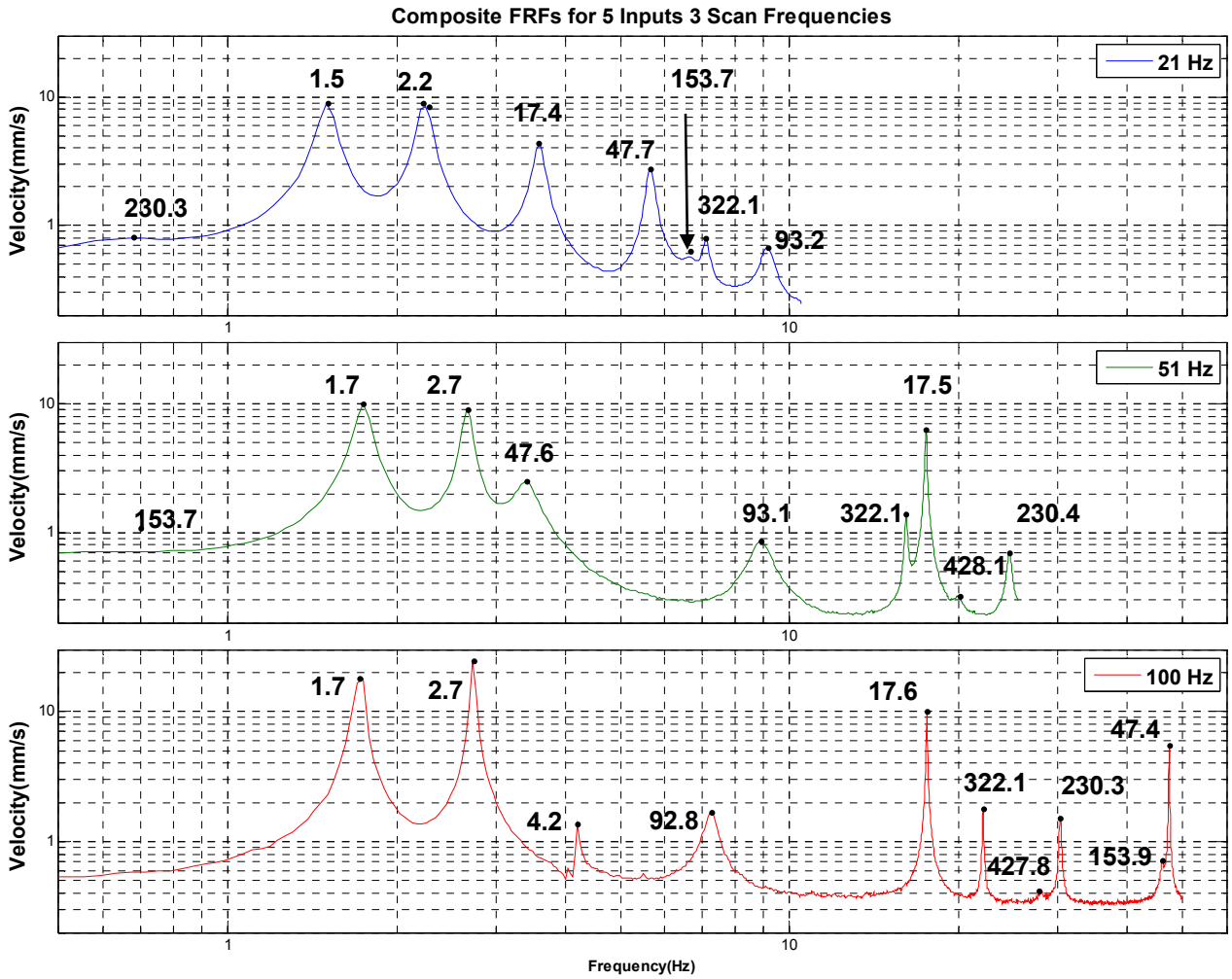

Figure 7: Composite average of pseudo-FRF matrices for 21, 51 and 100 Hz scanning frequencies.

Mode #, Bending Mode #	Analytical Freq. (Hz)	fscan = 21 Hz		fscan = 51 Hz		fscan = 100 Hz	
		Freq (Hz)	Aliased (Hz)	Freq (Hz)	Aliased (Hz)	Freq (Hz)	Aliased (Hz)
3, 1	17.6	17.4	3.6	17.5	17.5	17.6	17.6
4, 2	48.5	47.7	5.7	47.6	3.4	47.4	47.4
5, 3	95.1	93.2	9.2	93.1	8.9	92.8	7.3
6, 4	157.3	153.7	6.7	153.7	0.9	153.9	46.1
7, 5	234.9	230.3	0.7	230.4	24.6	230.3	30.3
8, 6	328.1	322.1	7.1	322.1	16.1	322.1	22.1
9, 7	436.9	-	-	428.1	20.1	427.8	27.8

Table 2: Natural frequencies of CSLDV data identified by AMI, unaliased and aliased, for three different scan frequencies.

At 21 Hz the scan frequency is 40 times lower than the ideal, and the effects of aliasing begin to make modal parameter identification difficult. At this frequency, the seventh bending mode, which should have been aliased to 8.7 Hz, is overwhelmed two more strongly excited modes, so it is not detected by the MIMO modal parameter identification algorithm. Depending on the particular modal parameter identification routine employed, this aliased mode might adversely affect the accuracy of the modal parameters identified for the neighboring modes. The Algorithm of Mode Isolation (AMI) [19], which was used in this work, is not particularly robust to missing modes, yet even then the mode shapes identified at 21 Hz are all quite accurate. These mode shapes are shown in Figure 8, compared with the analytical shapes. The shapes agree very well with the analytical shapes, and are very similar to the shapes identified from the 51 Hz data, except for the missing 7th mode.

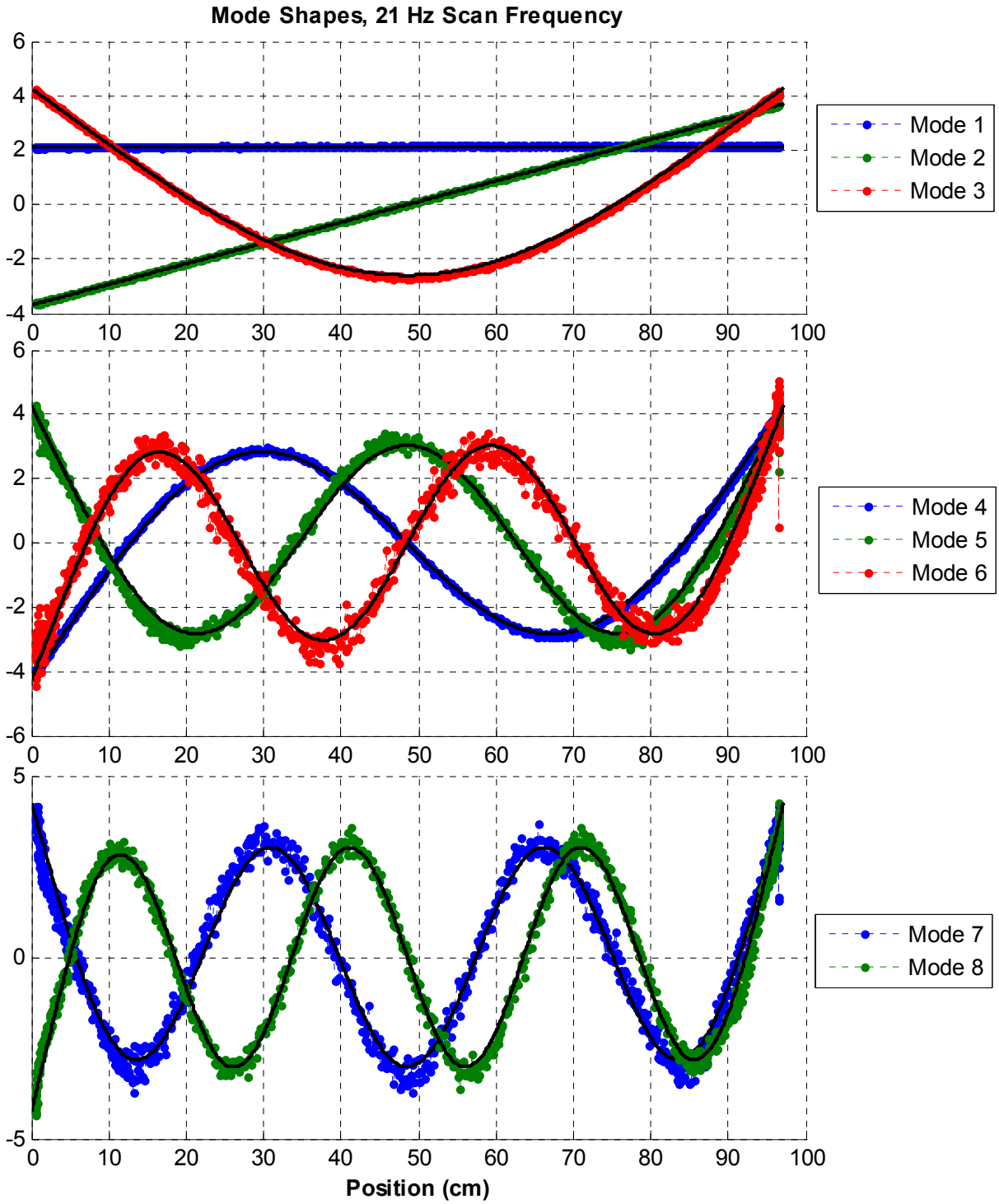

Figure 8: Mode shapes for free-free beam obtained experimentally using CSLDV with 21Hz scanning frequency, compared to analytical shapes. Solid black lines denote the analytical Euler-Bernoulli shape; dots show the experimentally obtained shapes at each pseudo-measurement point. The experimental mode vectors shown here were scaled to have the same norm as the analytical ones, so only the shapes of the vectors is of interest in this plot.

4. CONCLUSIONS

This work has demonstrated that the proposed CSLDV techniques can accurately identify the mode shapes of a structure at hundreds of spatial points simultaneously from just a few free responses. The difference in the measurement time is striking.

For the 51 Hz scanning frequency, the CSLDV method required only 2.5 minutes of vibration data to obtain the first seven bending modes of the structure at 402 points along the length of the beam. One would need 17 hours of vibration data to obtain an FRF matrix of the same size (402 outputs by 5 inputs) using conventional techniques! Realistically, the actual resolution in the measurements is governed by measurement noise, but the difference in test time remains very significant. It is even more significant to note that one is not likely to obtain mode shapes of similar quality using impact excitation with conventional scanning LDV because it is too difficult to control the input from hammer blow to the next, as was demonstrated in [12]. If the input source is a blast or some other kind of transient input that cannot easily be repeated or controlled, then conventional scanning LDV may not be applicable at all. The enhanced spatial resolution that CSLDV provides could potentially be used to more reliably calibrate finite element models, or to detect damage in low frequency structures.

A simple mass-normalization procedure was developed and demonstrated for a free-free beam. The procedure found scale factors for all of the modes of the beam that were no more than 20% different from the modes of an Euler-Bernoulli beam with nominal modulus, density and dimensions. Much of the discrepancy may be attributable to variation in the hammer blows and uncertainty in the damping estimates.

The Multiple Discrete Time Systems (MDTS) identification procedure, originally developed for Linear Time-Periodic systems, was applied to the CSLDV measurements and found to have some very significant advantages over existing techniques [1, 8, 11, 12]. The MDTS method allows one to use standard modal parameter identification routines to identify the modal natural frequencies, damping ratios and mode shapes of a structure from CSLDV measurements, so the methods are easy to master, especially if one is experienced with conventional modal testing. One can combine measurements from multiple inputs to create a MIMO data set, and standard tools such as the Complex Mode Indicator Function can be readily applied. Although not attempted here, Spatial Condensation could also be applied [13, 25] to reduce the computational burden required to identify modes from a data set consisting of hundreds or even thousands of response points and multiple input points. For the current work, this was not needed because the AMI algorithm was generally able to identify all of the modes of the structure in a reasonable amount of time even when dealing with hundreds of pseudo-measurement points simultaneously.

The proposed techniques are most effective when the CSLDV scan frequency is at least twice the maximum frequency of interest, because the modal frequencies are aliased otherwise. On the other hand, this paper demonstrated that good results could be obtained for this particular system even when the scan frequency was 10 or even 20 times lower than the maximum frequency of interest. The beam is lightly damped and its modes are well separated, so one would expect to have to use higher scan frequencies for a structure with more closely spaced modes or with heavy damping. Existing CSLDV techniques [1, 8, 11, 12] are most easily applied in the other extreme, when the scan frequency is much lower than the lowest frequency of interest and when the structure is lightly damped with well spaced modes. That approach may have presented some difficulty for this system because its fundamental natural frequency is only 17.6 Hz.

Scan frequencies ranging from 21 to 100 Hz were investigated. Similar mode shapes were obtained at each frequency, although aliasing at the lower scan frequencies made it impossible to extract the 7^{th} bending mode. It is important to note there was not a significant difference in the scatter of the mode shapes from 21 to 100 Hz (the 100 Hz shapes were not shown here, but were shown in [3]), nor in the quality of the composite FRF as the scan frequency varied. This at first seems to contradict Martarelli's findings [26], which show that speckle noise increases with increasing scanning frequency, but that work also reported that speckle noise was most severe at the scan frequency and its multiples (Rothberg has reported similar findings [20, 21]). Speckle noise away from the scan frequencies is much less severe. The MDTS method aliases the scan frequency and its multiples to the zero frequency line on the pseudo-FRFs, so speckle noise at those frequencies should have little effect on the results. In this work, the speckle noise was found to be small away from the scan frequencies and only seemed to affect one mode that was very weakly excited.

5. REFERENCES

[1] A. B. Stanbridge, M. Martarelli, and D. J. Ewins, "Scanning laser Doppler vibrometer applied to impact modal testing," in *17th International Modal Analysis Conference - IMAC XVII*, Kissimmee, FL, USA, 1999, pp. 986-991.

[2] A. B. Stanbridge, M. Martarelli, and D. J. Ewins, "Measuring area vibration mode shapes with a continuous-scan LDV," *Measurement,* vol. 35, pp. 181-9, 2004.

[3] M. S. Allen and M. W. Sracic, "A Method for Generating Pseudo Single-Point FRFs from Continuous Scan Laser Vibrometer Measurements," in *26th International Modal Analysis Conference (IMAC XXVI)*, Orlando, Florida, 2008.

[4] P. Sriram, J. I. Craig, and S. Hanagud, "Scanning laser Doppler vibrometer for modal testing," *International Journal of Analytical and Experimental Modal Analysis,* vol. 5, pp. 155-167, 1990.

[5] P. Sriram, S. Hanagud, and J. I. Craig, "Mode shape measurement using a scanning laser doppler vibrometer," *International Journal of Analytical and Experimental Modal Analysis,* vol. 7, pp. 169-178, 1992.
[6] P. Sriram, S. Hanagud, and J. I. Craig, "Mode shape measurement using a scanning laser doppler vibrometer," Florence, Italy, 1991, pp. 176-181.
[7] C. W. Schwingshackl, A. B. Stanbridge, C. Zang, and D. J. Ewins, "Full-Field Vibration Measurement of Cylindrical Structures using a Continuous Scanning LDV Technique," in *25th International Modal Analysis Confernce (IMAC XXV)*, Orlando, Florida, 2007.
[8] A. B. Stanbridge and D. J. Ewins, "Modal testing using a scanning laser Doppler vibrometer," *Mechanical Systems and Signal Processing,* vol. 13, pp. 255-70, 1999.
[9] M. Martarelli, "Exploiting the Laser Scanning Facility for Vibration Measurements," in *Imperial College of Science, Technology & Medicine*. vol. Ph.D. London: Imperial College, 2001.
[10] S. Vanlanduit, P. Guillaume, and J. Schoukens, "Broadband vibration measurements using a continuously scanning laser vibrometer," *Measurement Science & Technology,* vol. 13, pp. 1574-82, 2002.
[11] A. B. Stanbridge, A. Z. Khan, and D. J. Ewins, "Modal testing using impact excitation and a scanning LDV," *Shock and Vibration,* vol. 7, pp. 91-100, 2000.
[12] R. Ribichini, D. Di Maio, A. B. Stanbridge, and D. J. Ewins, "Impact Testing With a Continuously-Scanning LDV," in *26th International Modal Analysis Conference (IMAC XXVI)* Orlando, Florida, 2008.
[13] R. J. Allemang and D. L. Brown, "A Unified Matrix Polynomial Approach to Modal Identification," *Journal of Sound and Vibration,* vol. 211, pp. 301-322, 1998.
[14] M. Allen and J. H. Ginsberg, "Floquet Modal Analysis to Detect Cracks in a Rotating Shaft on Anisotropic Supports," in *24th International Modal Analysis Conference (IMAC XXIV)*, St. Louis, MO, 2006.
[15] M. S. Allen, "Floquet Experimental Modal Analysis for System Identification of Linear Time-Periodic Systems," in *ASME 2007 International Design Engineering Technical Conference*, Las Vegas, NV, 2007.
[16] M. S. Allen, "Floquet Experimental Modal Analysis for Identification of Linear Time-Periodic Systems," *Journal of Computational and Nonlinear Dynamics* vol. (submitted), 2008.
[17] H. Van Der Auweraer and J. Leuridan, "Multiple Input Orthogonal Polynomial Parameter Estimation," *Mechanical Systems and Signal Processing,* vol. 1, pp. 259-272, 1987.
[18] E. Balmes, "Integration of Existing Methods and User Knowledge in a MIMO Identification Algorithm for Structures with High Modal Densities," in *11th International Modal Analysis Conference (IMAC XI)*, Kissimmee, Florida, 1993, pp. 613-619.
[19] M. S. Allen, "Global and Multi-Input-Multi-Output (MIMO) Extensions of the Algorithm of Mode Isolation (AMI)," in *George W. Woodruff School of Mechanical Engineering* Atlanta, Georgia: Georgia Institute of Technology, 2005, p. 129.
[20] S. Rothberg, "Numerical simulation of speckle noise in laser vibrometry," *Applied Optics,* vol. 45, pp. 4523-33, 2006.
[21] S. J. Rothberg, "Laser vibrometry. Pseudo-vibrations," *Journal of Sound and Vibration,* vol. 135, pp. 516-522, 1989.
[22] S. J. Rothberg and B. J. Halkon, "Laser vibrometry meets laser speckle," Ancona, Italy, 2004, pp. 280-91.
[23] M. S. Allen and J. H. Ginsberg, "A Global, Single-Input-Multi-Output (SIMO) Implementation of The Algorithm of Mode Isolation and Applications to Analytical and Experimental Data," *Mechanical Systems and Signal Processing,* vol. 20, pp. 1090–1111, 2006.
[24] J. H. Ginsberg, M. S. Allen, A. Ferri, and C. Moloney, "A General Linear Least Squares SDOF Algorithm for Identifying Eigenvalues and Residues," in *21st International Modal Analysis Conference (IMAC-21)*, Orlando, Florida, 2003.
[25] R. J. Allemang, *Vibrations Course Notes*. Cincinnati: http://www.sdrl.uc.edu/, 1999.
[26] M. Martarelli and D. J. Ewins, "Continuous scanning laser Doppler vibrometry and speckle noise occurrence," *Mechanical Systems and Signal Processing,* vol. 20, pp. 2277-89, 2006.